

In this picture, the rest-frame ultraviolet emission seen at optical wavelengths comes from an "active" component of varying strength across the sample. Studies of the optical morphologies of these objects, including high resolution imaging by Hammer and Le Fèvre at CFHT, have revealed bizarre structures not encountered at low redshifts. The emission is frequently aligned along the axis of the radio source in blobs and elongated components. It is not yet known whether it is due to star-formation induced by the radio jet or whether it has a non-stellar origin. Regardless, this active component must be intimately associated with the active nucleus.

The present program was undertaken to study the infrared morphologies of high redshift radio galaxies to test the idea that the infrared light is dominated by a mature underlying galaxy, and if indeed it is, to then study this cosmologically important component. The results from the first phase of this project (to study a well-defined sample at $0.8 < z < 1.3$, mostly carried out on other telescopes but including our CFHT image of 3C65) has recently been submitted for publication. We find that, while the infrared images are in most cases still "aligned" with the radio source axis, this is a much weaker effect than that seen at optical wavelengths and is consistent with being produced by the long-wavelength "tail" of a roughly flat-spectrum active component underneath a much redder and symmetric "old-galaxy" component. Quantitative measures of the alignment indicate that typically only 10-20% of the infrared light can come from a component with the same morphological characteristics as the short wavelength ultraviolet light, with the remainder coming from a symmetric component.

In this context, 3C65 is especially interesting. It is the reddest radio galaxy known at these redshifts, and therefore presumably has least contamination from the active component associated with the nuclear activity. The high resolution and

depth of this image allows us to compare the scale size of this image with similar radio galaxies at lower redshifts. In Figure 15, we show the H-band surface brightness profile of 3C65. This follows a de Vaucouleur's $r^{1/4}$ law over a wide dynamic range. The derived effective radius (uncorrected for the effects of seeing) is $r_e = 1.0''$ or approximately 8.5 kpc for $q_0 = 0.5$. This value is close to the middle of the range of values of r_e found in low redshift radio galaxies.

Simon Lilly and Michael Rigler
Institute for Astronomy, University of Hawaii

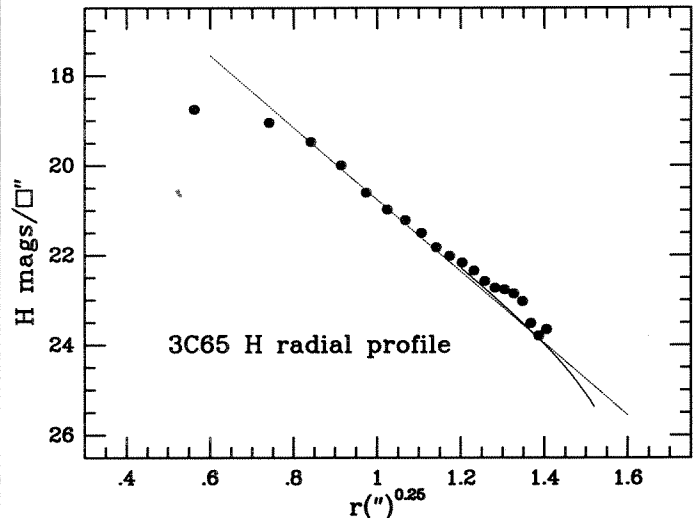


Figure 15: Surface brightness profile of 3C65 in the H-band, showing the reasonable fit to a de Vaucouleurs profile. Points represent observed surface brightness in annuli, curve represents a polynomial profile fitted to the outer regions of the galaxy. Dashed line indicates a de Vaucouleurs profile with $r_e = 1.0''$ (8.6 kpc).

High Resolution Imaging of the Young Star DD Tauri

In the last 5 years, evidence has accumulated for the existence of circumstellar disks around young stars. With a typical radius of 100 AU, these optically thick, presumably protoplanetary disks cover only a fraction of an arcsec on the sky, even at the distance of the nearest stellar formation regions (e.g., Taurus, $d=150\text{pc}$). High-resolution imaging techniques are therefore required to directly detect them.

With this goal in mind, we started a long-term program at CFHT dedicated to optical and near-IR high-resolution imaging of T Tauri stars, a class of very active, low-mass pre-main sequence stars. We report here preliminary results obtained on DD Tauri, which we found to possibly be surrounded by a circumstellar disk seen at high inclination.

Figure 16a shows contours from the first high-resolution image of DD Tau we obtained in October 1990 using the DAO High Resolution Camera at the telescope prime focus. The image was taken through a narrow-band filter ($\Delta\lambda=100\text{\AA}$) centered on $H\alpha$ with an exposure time of 10 seconds.

The object appears clearly resolved with two intensity peaks separated by $0.55 \pm 0.05''$ at $P.A.=186 \pm 3^\circ$. A narrow-band image centered on the continuum next to $H\alpha$ was kindly obtained a few days later by O. Le Fèvre with FOCAM and

confirmed the N-S elongation of the object, though the seeing was not good enough to clearly resolve it.

These results prompted us to perform near-IR speckle observations of DD Tau during our December 1990 run using the Observatoire de Paris-INSU CIRCUS IR camera. Under good seeing conditions, 600 images of DD Tau were obtained in the L' band ($3.8\mu\text{m}$) using a $0.1''/\text{pixel}$ spatial sampling and a 700ms exposure time. The individual images were recentered on the brightest pixel and co-added to yield the reconstructed image shown in Figure 16b, while the 2D visibilities are shown in Figure 16c.

The visibilities, i.e., the modulus of the 2D Fourier transform of the object, indicate a cut-off frequency of 3 arcsec^{-1} and exhibit a clear ripple pattern characteristic of binary stars. The object is thus well resolved at L with a separation of $0.53 \pm 0.05''$ at $P.A.=183 \pm 3^\circ$, a result consistent with that found from optical images.

The most straightforward interpretation of the high-resolution images is to assume that DD Tau is a binary, an already interesting result in itself since only a handful of sub-arcsecond pre-main sequence binaries have been detected to date. Alternatively, the two intensity peaks might correspond to stellar photons scattered above and below the plane of a circumstellar disk seen nearly edge-on. Little direct starlight would then reach the observer due to high obscuration by the optically thick disk.

Support to the disk interpretation is provided by the unusual forbidden lines profiles of DD Tau. Active pre-main sequence

stars, similar to DD Tau, usually exhibit forbidden lines profiles ([OI], [SII], [NII]) that are systematically blueshifted relative to the stellar rest velocity. These lines form in the outer parts of a bipolar wind, and if both the receding and approaching lobes of the wind were seen, a redshifted and blueshifted component would appear in the line profile. The lack of redshifted emission in the observed line profiles is usually interpreted as indicating that only the approaching part of the wind is seen, while the receding part of it is obscured by an opaque circumstellar disk in the equatorial plane.

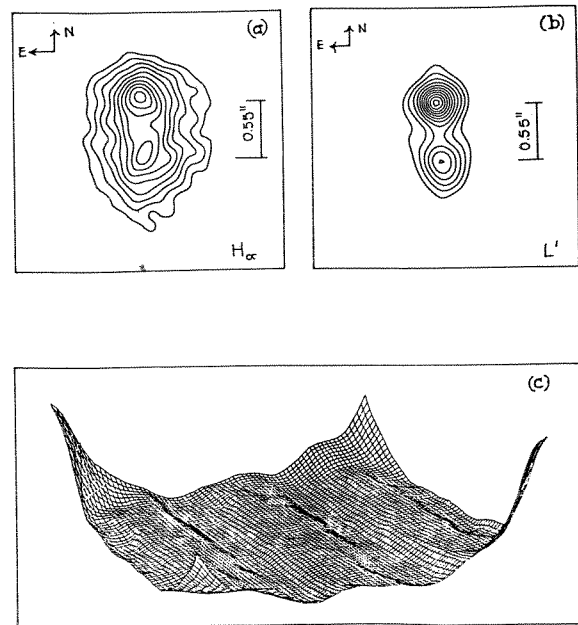
The [NII] $\lambda 6584$ line profile of DD Tau, however, exhibit two peaks, one being blueshifted and the other redshifted relative to the star's rest velocity, which suggests that the disk is seen at high inclination.

A crucial test to whether the disk or the binary interpretations are correct will be provided by a high-resolution, long-slit spectrum along P.A. = 6° . In the framework of the disk hypothesis, blueshifted forbidden line profiles are associated to one intensity peak and the redshifted ones to the other. This and other observations are currently being planned. Meanwhile, the near-IR speckle images (obtained two nights before this preliminary report is written) will be more fully processed and analyzed.

J. Bouvier, E. Tessier, and C. Perrier

Figure 16: Contours from the $H\alpha$ image (a) and from the $3.8 \mu\text{m}$ shift-and-add image (b) of DD Tauri. The lowest contour corresponds to 1/4 of the maximum value; (c) the 3D representation of the 2D visibilities at $3.8 \mu\text{m}$. A characteristic ripple pattern (periodicity = 2 arcsec^{-1}) is clearly apparent along the N-S direction. The noise strongly increases beyond the cut-off frequency located at 3 arcsec^{-1} from the center.

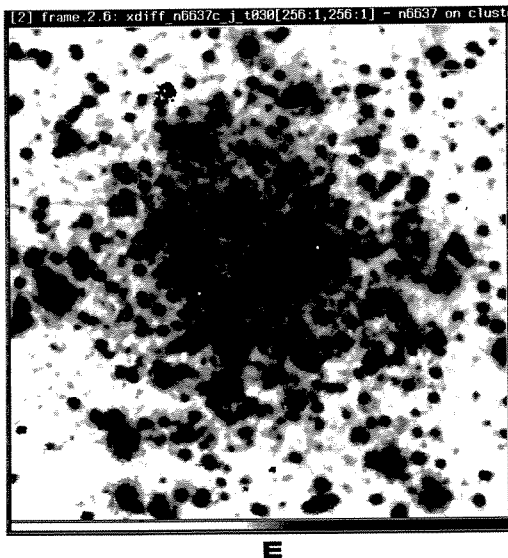
DD Tauri



Near-Infrared Photometry of Bright Giants in M69 Using the UH NICMOS Array

The introduction of large-format low-noise infrared arrays promises to have a major impact on observational astronomy, similar in extent to that experienced in the 1970's when CCD's

first became available. The Rockwell NICMOS 3 array, which consists of $40 \mu\text{m}$ pixels in a 256^2 format, is one the largest infrared detectors currently available. During a recent discretionary night in September 1990, we used this device to obtain a series of short J, H, and K exposures of the central regions of the globular cluster M69; the final J image is shown in Figure 17. The data were obtained to investigate the position of the giant branch locus in this cluster, as previous near-infrared aperture measurements suggest that the giant branch of M69 may be exces-



←
Fig. 17 (left): J image of the center of M69. Exposure time = 9 sec.

⇒
Fig. 18 (right): (K, J-K) CMD of Field shown in Figure 15. The M69 data are shown as crosses while data for 47 Tuc are shown as solid squares. The solid and open triangles in the upper left hand corner show the effects on the 47 Tuc data of changing the B-V color excess of M69 from 0.17 to 0.10.

